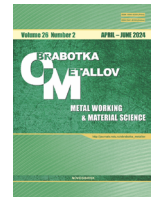




# Obrabotka metallov - Metal Working and Material Science





Journal homepage: [http://journals.nstu.ru/obrabotka\\_metallov](http://journals.nstu.ru/obrabotka_metallov)



## The study of vibration disturbance mapping in the geometry of the surface formed by turning

Vilor Zakovorotny<sup>a</sup>, Valery Gvindjiliya<sup>b,\*</sup>

Don State Technical University, 1 Gagarin square, Rostov-on-Don, 344000, Russian Federation

<sup>a</sup>  <https://orcid.org/0000-0003-2187-9897>,  [vzakovorotny@dstu.edu.ru](mailto:vzakovorotny@dstu.edu.ru); <sup>b</sup>  <https://orcid.org/0000-0003-1066-4604>,  [vvgvindjiliya@donstu.ru](mailto:vvgvindjiliya@donstu.ru)

### ARTICLE INFO

#### Article history:

Received: 20 December 2023

Revised: 22 February 2024

Accepted: 20 March 2024

Available online: 15 June 2024

#### Keywords:

Transformation of vibrations into the relief of the workpiece  
Trajectories of forming movements  
Dynamic cutting system

#### Funding

The study was supported by a grant within the framework of the «Nauka-2030».

### ABSTRACT

**Introduction.** The development of virtual digital models of the machining process on metal-cutting machines is a dynamically developing direction of increasing the efficiency of machine-building production. Such models include subsystems of parts quality prediction. Accuracy and validity of its work directly depends on the built model of dynamic cutting system, which is perturbed by force noise, the sources of which have different physical origin. In addition, the autonomous dynamic system itself is a generator of various attracting sets of deformations, such as limit cycles or chaotic attractors. Taking into account various nonlinear transformations in the properties of the dynamics of the cutting process allows increasing the adequacy of the model to the real process and is an actual task in the construction of simulation modeling systems of the dynamics of surface machining by cutting. **Study object.** Our earlier studies allow us to determine the geometry corresponding to the deformation trajectories of the surface formed by cutting. However, the adequacy of the mapping of the calculated trajectories to the geometry estimates remains not quite clear. The proposed paper focuses on achieving an adequate mapping of calculated as well as measured strain trajectories into the geometric topology of the part. **The aim of the work** is to evaluate the mapping of vibration perturbations of the system into the geometry of the surface formed by cutting. **Method and methodology.** The research is of experimental-theoretical nature. The content of the research includes the study of the correspondence of frequency characteristics obtained on the model and in real machining. The main attention is paid to the mapping of deformations to the part geometry. For this purpose, the paper considers the coherence functions between the strain functions and the part profile. **Results and Discussion.** It is shown that the conditioning of these transformations has a limited frequency range in which the explanation of the variable components of the generated relief is statistically significant. Mathematical modeling of the dynamic cutting system based on the mechanics of interaction between tool and workpiece allows adequate prediction of the macro geometry of the part formed by cutting. The obtained mathematical tools can be used to create systems for predicting the geometry of the machined surface.

**For citation:** Zakovorotny V.L., Gvindjiliya V.E. The study of vibration disturbance mapping in the geometry of the surface formed by turning. *Obrabotka metallov (tehnologiya, oborudovanie, instrumenty) = Metal Working and Material Science*, 2024, vol. 26, no. 2, pp. 107–126. DOI: 10.17212/1994-6309-2024-26.2-107-126. (In Russian).

## Introduction

In the last decade, many scientific teams have been working towards the creation of a virtual model of the machining process on metal cutting machines, i.e., the creation of its digital twin. The machining process is considered as a system, the individual subsystems of which are united by various links [1–7]. In the CNC machine tool system the subsystems that reveal the accuracy of correspondence between the program-defined and real motion trajectories of executive elements are singled out [8–10]. Attention is paid to the identification of generalized masses and friction links in servo drives of machine tool actuators, its influence on the correspondence between the trajectories specified by the program and real trajectories and the accuracy of interpolation and reproduction of trajectories [11–16]. The direction of building a virtual

#### \* Corresponding author

Gvindjiliya Valery E., Ph.D. (Engineering), Senior Lecturer  
Don State Technical University,  
1 Gagarin square,  
344000, Rostov-on-Don, Russian Federation  
Tel.: +7 918 583-23-33, e-mail: [vvgvindjiliya@donstu.ru](mailto:vvgvindjiliya@donstu.ru)

model of the machining process on the machine tool, based on the intellectual approach to model building, which reveals the relationship between technological modes and output parameters of the cutting process, considered in the unity of the quality of parts manufacturing and machining efficiency [17–21], has also been formed. At the same time, the content of these transformations is not disclosed. Efficiency is also evaluated on the basis of determining the cutting speed, at which the tool wear intensity is minimal. When solving this issue, the choice of technological modes is considered, for example, according to the criterion of optimal cutting temperature [22–25]. The quality of the models depends on the depth of consideration of all the factors affecting the process.

The important problem in building a virtual model is to ensure the required motion trajectory of the tool tip relative to the workpiece, taking into account its elastic deformations, as well as its transformation into the geometric topology of the surface formed by cutting. Its solution is based on studies of the *dynamic cutting system (DCS)*, the study of which has been carried out since the mid-50s-60s of the last century [26–28]. The idea of a *DCS* consisting of subsystems of the tool and the workpiece, which are united by a link formed by cutting [29–32], was formed. This coupling is a model of the forces represented in the state coordinates. The modeling of forces takes into account the regeneration of the trace on the workpiece left by the deformations in the previous revolution [33–36]. A bifurcation analysis of the stability of the cutting process in “trace” machining and a process analysis based on finite element modeling are given [37–40]. The lag of force variations during changes in the cutting area is taken into account [29, 41–46]. Nonlinear dependences of cutting and friction forces on velocities and displacements are taken into account [47–54]. Parametric self-excitation is considered [55–57]. This list does not exhaust the publications on *DCS*. It considers the stability of trajectories and the formation of various attracting sets of deformations (limit cycles, invariant tori, chaotic attractors, etc.).

However, the problem of its transformation into the geometry of the part formed by cutting remains open. **The purpose of this paper** is to investigate the mechanism of transformation of deformation displacements of the tool into the geometry of the workpiece taking into account vibration disturbances in the dynamics of the turning cutting process in various machining conditions and modes. The paper evaluates the adequacy of the deformations calculated by the simulation model and measured during the real experiment, as well as its transformation into the geometrical topology of the workpiece. The adequacy is determined based on the proximity of the spectra as well as coherence functions. The research allows us to determine the adequacy of part geometry formation by forming motion trajectories (*FMT*), which are the unity of trajectories of machine actuators and deformation displacements of the tool relative to the workpiece.

## Research technique

### *Mathematical description of the dynamic system*

The following transformations in the cutting system should be considered as the basis for building a numerical model. The first is the transformation of the trajectories defined in the *CNC* system in the form of the control vector  $U = \{U_1, U_2, U_3\}^T \in \mathfrak{R}_U^{(3)}$  into the trajectories of the machine actuating elements (*TMAE*). The *TMAE* space for a lathe is given by the vector  $L = \{L_1, L_2, L_3\}^T \in \mathfrak{R}^{(3)}$  (fig. 1, a). Here  $L_1(t)$  and  $L_2(t)$  are movements of transverse and longitudinal calipers;  $L_3(t) = \pi \int_0^t \Omega(\xi) D(\xi) d\xi$  is the movement of the workpiece along the direction  $L_3$ . The velocities are also set as  $dL / dt = V(t) = \{V_1, V_2, V_3\}^T \in \mathfrak{R}^{(3)}$ . The transformation  $\mathfrak{R}_U^{(3)} \Rightarrow \mathfrak{R}^{(3)}$  is not considered in this study. The trajectories  $L$  and  $V$  are assumed to be set within the bandwidths of the servomotors. Thus, the trajectories  $L$  and  $V$  describe the ideal contour of the workpiece.

Secondly, it is necessary to find out the transformation of the trajectories  $L$  and  $V$  into forming motion trajectories (*FMT*)  $L^{(\Phi)} = \{L_1^{(\Phi)}, L_2^{(\Phi)}, L_3^{(\Phi)}\}^T \in \mathfrak{R}^{(3)}$  and  $V^{(\Phi)} = dL^{(\Phi)} / dt = \{V_1^{(\Phi)}, V_2^{(\Phi)}, V_3^{(\Phi)}\}^T \in \mathfrak{R}^{(3)}$ .

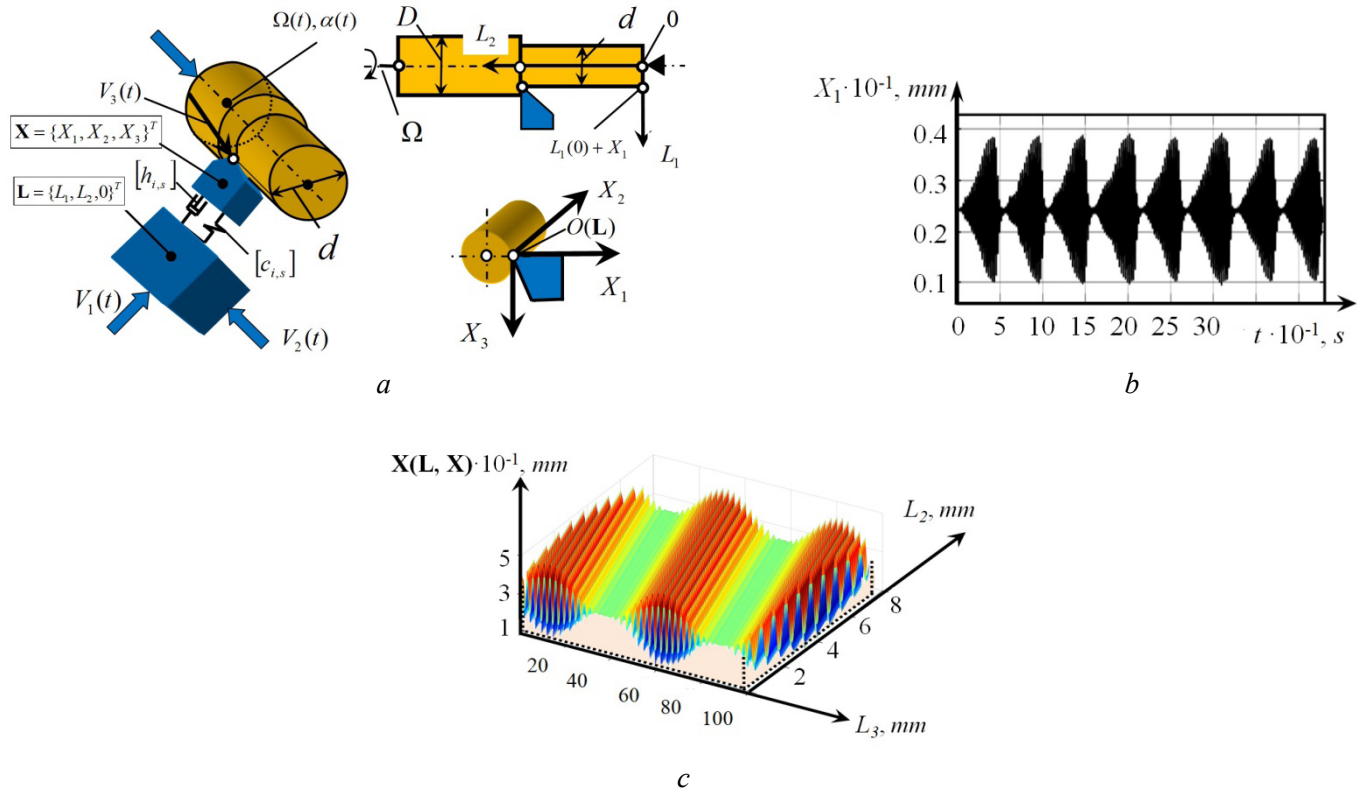


Fig. 1. Scheme for the formation of state space coordinates (a), and an example of “skeleton” geometrical topology (c) for variations of deformation displacements with frequency equal to the workpiece rotation frequency (b)

The trajectories  $\mathbf{L}^{(\Phi)}$  and  $\mathbf{V}^{(\Phi)}$  take into account the deformations of the tool tip in addition to the *TMAE*. In the present study, we will focus on the case of machining an absolutely rigid workpiece by longitudinal turning. Then

$$\begin{cases} \mathbf{L}^{(\Phi)} = \mathbf{L} - \mathbf{X}(\mathbf{L}); \\ \mathbf{V}^{(\Phi)} = \mathbf{V} - \mathbf{v}(\mathbf{L}), \end{cases} \quad (1)$$

where  $\mathbf{X} = \{X_1, X_2, X_3\}^T \in \mathfrak{R}_{\mathbf{X}}^{(3)}$ ,  $\mathbf{v} = \{v_1, v_2, v_3\}^T \in \mathfrak{R}_{\mathbf{X}}^{(3)}$  are the vectors of deformations  $\mathbf{X}$  and its velocities  $\mathbf{v} = d\mathbf{X} / dt$  considered in the moving coordinate system given by  $\mathbf{L}$  (fig. 1, a).

Let's consider turning the shaft  $D = const$  with constant cutting modes:  $\mathbf{L} = \{L_1 = d / 2, L_2 = V_2 t, L_3 = \pi d \Omega\}^T$ .

Thirdly, it is necessary to study the pattern of transformation  $\mathbf{L}^{(\Phi)}$  and  $\mathbf{V}^{(\Phi)}$  into geometrical surface topology  $\mathfrak{S}(\mathbf{L}, \mathbf{R})$ . Geometrical topology is a mapping of shaft surface irregularities into a bounded plane. In the plane, the length of the shaft circumference along the  $L_3$  axis, the length of the shaft along the longitudinal feed direction along the  $L_2$  axis, and the variations of the radius of the vector  $\mathbf{R}$  in the form of irregularities along the  $L_1$  axis. If the deformations are  $\mathbf{X} = 0$ , then  $\mathfrak{S}(\mathbf{L}, \mathbf{R})$  is the plane  $\langle L_2 - L_3 \rangle$ .

Let us also consider a point mapping of the tool vertex constructed in a similar way. Let us call such a mapping a “skeletal” geometric topology  $\mathfrak{S}_c(\mathbf{L}, \mathbf{X})$ . Fig. 1, c shows its example for the vector  $\mathbf{X}$ . The function  $X_1(t)$  characterizes the height irregularities (fig. 1, c),  $X_2(t)$  and  $X_3(t)$  are stepwise. If the dynamical system is stable and unperturbed, the deformations are  $\mathbf{X}^* = \{X_1^*, X_2^*, X_3^*\}^T \in \mathfrak{R}_{\mathbf{X}}^{(3)}$ . This is the equilibrium point. It is shifted relative to  $\mathbf{L}$  by a constant value  $\mathbf{X}^*$ . If  $\mathbf{L} = \{L_1 = d / 2, L_2 = V_2 t, L_3 = \pi d \Omega\}^T$ , then  $\mathfrak{S}_c(\mathbf{L}, \mathbf{X})$  represents the plane parallel to  $\langle L_2 - L_3 \rangle$ , and shifted upward along the axis  $L_1$  by the value  $X_1^* = const$ . If the geometrical topology  $\mathfrak{S}(\mathbf{L}, \mathbf{R})$  formed by cutting along a point contour is  $\mathfrak{S}_c(\mathbf{L}, \mathbf{X})$ , then

it is accurately formed by the trajectories  $L^{(\Phi)}$ . Then observation and/or calculation of  $L^{(\Phi)}$  allows to accurately predict  $\mathfrak{S}(L, R)$ . If vector  $L$  is defined and its accuracy is ensured by the CNC system, then to determine  $\mathfrak{S}_c(L, X)$  it is necessary to calculate  $X$ . For this purpose we can use the developed mathematical models [22, 23, 45, 46, 54, 55, 58, 61]. Then

$$\left\{ \begin{array}{l} m \frac{d^2 X}{dt^2} + h \frac{dX}{dt} + cX = F(L, V, X); \\ F = F^{(0)} \{\chi_1, \chi_2, \chi_3\}^T; \\ T^{(0)} dF^{(0)} / dt + F^{(0)} = \rho \{1 + \mu \exp[-\zeta(V_3 - v_3)]\} [t_P^{(0)} - X_1] \int_{t-T}^t \{V_2(\xi) - v_2(\xi)\} d(\xi), \end{array} \right. \quad (2)$$

where  $m, h, c$  are symmetric and positively definite matrices, i.e. potential matrices;  $\rho$  is a chip pressure on the leading edge of the tool;  $T^{(0)}$  is a chip time constant, that takes into account transients in the cutting zone;  $\mu, \zeta$  are parameters determining the dependence of forces on cutting speed;  $\chi_i, i = 1, 2, 3$  is an angular coefficient of cutting force orientation;  $t_P^{(0)}$  is a depth of cut without elastic deformations;  $T$  is a workpiece turnover time, i.e.

$$T(v_3, \Omega) = \int_{L_3^{(\Phi)} - \pi D}^{L_3^{(\Phi)}} \frac{d\xi}{\{V_3(\xi) - v_3(\xi)\}}. \quad (3)$$

System (2) is valid for small deformations in the vicinity of equilibrium, when the forces acting on the auxiliary flanks of the tool can be neglected. At large deviations of coordinates from equilibrium, it is necessary to take into account all nonlinear relationships and to introduce the interactions between the auxiliary flanks of the tool and the workpiece into the forces, as suggested in our earlier studies [22, 23, 45, 46, 54–61].

### Adequacy of the “base” model

Let us first consider the adequacy of the deformations mapping  $X$  in a “base” model in which the forces are perturbed by a “white” noise of low intensity  $\varphi(t)$ . The case when  $X^*$  is asymptotically stable is analyzed here. The point  $X^*$  corresponds to  $F^{(0,*)}$ . In view of the smallness of  $\varphi(t)$  it is sufficient to consider the linearized system (2) in variations with respect to equilibrium. For this purpose, let's make a substitution:  $X(t) = X^* + x(t)$ ,  $F_{(0)}^{(t)} = F^{(0,*)} + f(t)$ . The equation in variations relative to  $X^* = const$ ,  $F^{(0,*)} = const$ , and is obtained. Then the linearized Laplace equation in images is obtained

$$mp^2 z + hpz + cz = \varphi(p), \quad (4)$$

where  $z(p) = \{x_1(p), x_{21}(p), x_3(p), f(p)\}^T$ ;  $\varphi(p) = \{0, 0, 0, \varphi(p)\}$ ;  $p$  is a Laplace transform symbol;  $t_P^* = t_P^{(0)} - X_1^*$ ;

$$m = \begin{bmatrix} m & 0 & 0 & 0 \\ 0 & m & 0 & 0 \\ 0 & 0 & m & 0 \\ 0 & 0 & 0 & 0 \end{bmatrix}; \quad h = \begin{bmatrix} h_{1,1} & h_{2,1} & h_{3,1} & 0 \\ h_{1,2} & h_{2,2} & h_{3,2} & 0 \\ h_{1,3} & h_{2,3} & h_{3,3} & 0 \\ 0 & 0 & \rho\mu\zeta t_P^* S_P^{(0)} & T^{(0)} \end{bmatrix};$$

$$c = \begin{bmatrix} c_{1,1} & c_{2,1} & c_{3,1} & -\chi_1 \\ c_{1,2} & c_{2,2} & c_{3,2} & -\chi_2 \\ c_{1,3} & c_{2,3} & c_{3,3} & -\chi_3 \\ \rho[1 + \mu e^{-\zeta V_3}] S_P^{(0)} & \rho[1 + \mu e^{-\zeta V_3}] t_P^* & 0 & 1 \end{bmatrix}.$$

From (4) we calculate the autospectra of oscillations  $S_{x_1, x_1}(\omega)$ ,  $S_{x_2, x_2}(\omega)$ ,  $S_{x_3, x_3}(\omega)$ . For example, the spectrum of deformations  $X_I$  responsible for the height irregularities of the topology  $\mathfrak{S}_c(L, X)$  is

$$S_{X_1, X_1}(\omega) = W(p)W(-p)_{p=j\omega} \quad (5)$$

where

$$W(p) = \Delta_{X_1}(p) / \Delta(p);$$

$$\Delta_{X_1}(p) = \begin{bmatrix} (h_{2,1}p + c_{2,1}) & (h_{3,1}p + c_{3,1}) & -\chi_1 \\ (mp^2 + h_{2,2}p + c_{2,2}) & (h_{3,2}p + c_{3,2}) & -\chi_2 \\ (h_{2,3}p + c_{2,3}) & (mp^2 + h_{3,3}p + c_{3,3}) & -\chi_3 \end{bmatrix};$$

$$\Delta(p) = \begin{bmatrix} (mp^2 + h_{1,1}p + c_{1,1}) & (h_{2,1}p + c_{2,1}) & (h_{3,1}p + c_{3,1}) & -\chi_1 \\ (h_{1,2}p + c_{1,2}) & (mp^2 + h_{2,2}p + c_{2,2}) & (h_{3,2}p + c_{3,2}) & -\chi_2 \\ (h_{1,3}p + c_{1,3}) & (h_{2,3}p + c_{2,3}) & (mp^2 + h_{3,3}p + c_{3,3}) & -\chi_3 \\ \rho[1 + \mu e^{-\zeta V_3}]S_p^{(0)} & \rho[1 + \mu e^{-\zeta V_3}]t_p^* & -\rho\mu\zeta t_p^* S_p^{(0)} & 1 + pT^{(0)} \end{bmatrix};$$

$$t_p^* = t_p^{(0)} - X_1^*.$$

Experiments show that a dynamical system under real conditions is always perturbed. If the equilibrium is stable, then small perturbations correspond to a sequence satisfying the hypotheses of stationary randomness  $X_1^{(U)}(t)$ . Let the measured signal  $X_I^{(U)}(t)$  is a sequence  $X_I^{(u)}(t) = \{X_1^{(U)}(0), X_1^{(U)}(\Delta t), X_1^{(U)}(2\Delta t), \dots, X_1^{(U)}(s\Delta t)\}^T$ . Here  $(\Delta t)^{-1}$  is the Nyquist frequency. It is determined by an order of magnitude higher than the upper natural frequency of the oscillating circuits. The sequence  $X_I^{(U)}(t)$  allows to calculate the autocorrelation function and its Fourier image, i.e. spectrum  $S_{X_1^{(U)}, X_1^{(U)}}(\omega)$

$$S_{X_1^{(U)}, X_1^{(U)}}(\omega) = W^{(U)}(p)W^{(U)}(-p)_{p=j\omega}. \quad (6)$$

To assess the quality of model (4), we can introduce a proximity estimator

$$\wp_{X_S, X_S}^{(i)}(\omega) = \left\{ \tilde{S}_{X_S, X_S}^{(i)}(\omega) - \tilde{S}_{X_S^{(U)}, X_S^{(U)}}(\omega) \right\}^2, \quad \omega \in \left( 0, \frac{1}{\Delta t} \right), \quad i = 1, 2; s = 1, 2, 3, \quad (7)$$

where  $\tilde{S}_{X_S, X_S}^{(i)}(\omega) = \frac{1}{\Delta\omega} \int_{\tilde{u}-\tilde{\Delta u}}^{\tilde{u}} S_{X_S, X_S}^{(i)}(\omega) d\omega$ ;  $\tilde{S}_{X_S^{(U)}, X_S^{(U)}}(\omega) = \frac{1}{\Delta\omega} \int_{\tilde{u}-\tilde{\Delta u}}^{\tilde{u}} S_{X_S^{(U)}, X_S^{(U)}}(\omega) d\omega$  – moving

averages in the frequency window  $\Delta\omega$ ; spectrum  $S_{X_S^{(1)}, X_S^{(1)}}(\omega)$  is calculated by the formula (5); spectrum

$S_{X_S^{(2)}, X_S^{(2)}}(\omega)$  refers to the time sequence derived from the transformed “white” noise; frequency window  $\Delta\omega$  is selected substantially less than the bandwidth of oscillating circuits.

Finally, the adequacy analysis used amplitude-frequency characteristics measured directly on model (2) when the system is excited by forces  $\varphi_0 \sin(\omega t)$  with slowly varying frequency  $\omega$ . The obtained frequency response corresponds to  $S_{X_S^{(1)}, X_S^{(1)}}(\omega) = A_S^2(\omega)$  (fig. 4). Here  $A$  is the ratio of the amplitude at the output to the amplitude at the input. We can also consider the dispersion estimation in the frequency domain



$$\sigma_{X_S, X_S}^{(i)} = \left\{ \int_0^{\omega_\infty} \left[ S_{X_S, X_S}^{(i)}(\omega) - S_{X_S^{(u)}, X_S^{(u)}}(\omega) \right]^2 d\omega \right\} \times \left\{ \int_0^{\omega_\infty} \left[ S_{X_S^{(u)}, X_S^{(u)}}(\omega) \right]^2 d\omega \right\}^{-1}, \quad i = 1, 2; \quad s = 1, 2, 3, \quad (8)$$

where  $\omega_\infty$  is the frequency that is an order of magnitude higher than the upper natural frequency of the oscillating contour of the tool subsystem.

When analyzing adequacy, it is necessary to consider also the evaluation of the influence of additional interactions not included in the mathematical description of the model (2). For example, adhesive interactions, formation of dissipative structures (e.g., growth), and additional disturbances (e.g., kinematic disturbances from the machine itself). Moreover, these perturbations can be applied not directly to the forces, but to other elements of the system, in the case of kinematic perturbations – these are variations in feed rate. For this purpose, the coherence function between the observed strain displacements  $X_1^{(u)}(t)$  and the calculated  $X_1(t)$  is considered. Then

$$K_{X_S, X_S^{(u)}}^2(\omega) = \frac{1}{1 + \delta_S(\omega)}, \quad s = 1, 2, 3, \quad (9)$$

where  $\delta_S(\omega) = \frac{S_{\theta, S}(\omega)}{|W_S^{(u)}(j\omega)|^2}$ ;  $S_{\theta, S}(\omega)$  is spectrum of additional unmeasured noise;  $|W_S^{(u)}(j\omega)|^2$  is square of the modulus of transformation of “white” noise into deformations  $X_S^{(u)}(t)$ .

Equation (9) shows that the coherence function tends to unity in two cases: there are no additional interaction forces unaccounted for in the model or the unaccounted for interactions with respect to the accounted perturbations are small. Estimates (7)–(9) also allow us to perform a terminal correction of the parameters of model (2).

Let's consider an example of analyzing the adequacy of the model for small oscillations during longitudinal turning on a *IK62* machine tool (fig. 2). The *20X* steel shaft  $D = 20$  mm was machined with a tool equipped with non-transferable *T15K6* tetrahedral plates. Generalized mass was equal to  $0.015 \text{ kg}\cdot\text{s}^2/\text{mm}$ . The parameters are given in Table 1 and Table 2, determined according to the methodology described in [22, 23, 61]. Rotational speed of the workpiece was equal to 25 Hz. The corresponding cutting speed was equal to 1.5 m/s. Cutting depth and feed rate were equal:  $t_p^{(0)} = 2$  mm;  $S_p^{(0)} = 0.1$  mm.



a



b

Fig 2. General views of the equipment (a) and measurement interface (b) used for experiments

Table 1

**Dynamic link options**

$\rho, \text{ kg/mm}^2$	$\sigma, (\text{mm/s})^{-1}$	$T^{(0)}, \text{ s}$	$\mu$	$\chi_1$	$\chi_2$	$\chi_3$	$\Omega, \text{ s}^{-1}$
200–1.000	0.0011	0.0002	0.5	0.4	0.51	0.76	5–50

Parameters of the matrices of velocity coefficients and elasticity of the tool subsystem

$h_{1,1}$ , kg·s/mm	$h_{2,2}$ , kg·s/mm	$h_{3,3}$ , kg·s/mm	$h_{1,2}=h_{2,1}$ , kg·s/mm	$h_{1,3}=h_{3,1}$ , kg·s/mm	$h_{2,3}=h_{3,2}$ , kg·s/mm
1.3	1.1	0.8	0.6	0.5	0.4
$c_{1,1}$ , kg/mm	$c_{2,2}$ , kg/mm	$c_{3,3}$ , kg/mm	$c_{1,2}=c_{2,1}$ , kg/mm	$c_{1,3}=c_{3,1}$ , kg/mm	$c_{2,3}=c_{3,2}$ , kg/mm
2.000	900	350	200	150	80

Two sets of time sequences were considered: those calculated using the model parameters and those actually measured. General views of the experimental stand for research and the instrument equipped with sensors for vibration measurement are shown in fig. 2.

The “white” noise model of power disturbances in the frequency range up to 30.0 kHz was used to determine the calculated time sequences. Examples of time realizations of “white” noise, computed and measured time sequences  $X_I$  in the direction are shown in fig. 3.

In fig. 4 shows examples of spectra normalized to dispersion determined from the calculated  $S_{X_S, X_S}^{(2)}(\omega)$  (a) and measured  $S_{X_S^{(U)}, X_S^{(U)}}(\omega)$  (b) sequences. The analytically calculated spectra are also shown in red color on the graphs  $S_{X_S, X_S}^{(1)}(\omega)$ , and also in fig. 4, c shows a fragment of force perturbation in the form of sinusoidal change of additional forces with slowly changing frequency. In addition, an example of strain amplitude variations in the direction of  $X_1$ , i.e., the amplitude-frequency response of the model, is given (fig. 4, c). It should be noted that these characteristics remain unchanged at small amplitudes of force excitation. In the example under consideration, variations in the amplitude of the force disturbance up to 10 kHz do not change it. When the amplitude increases, the nonlinear properties of the model are noticeable. It is manifested in changes in the resonance frequency, in the redistribution of frequencies and amplitudes of the main oscillators, in the broadening of its spectral line, and so on.

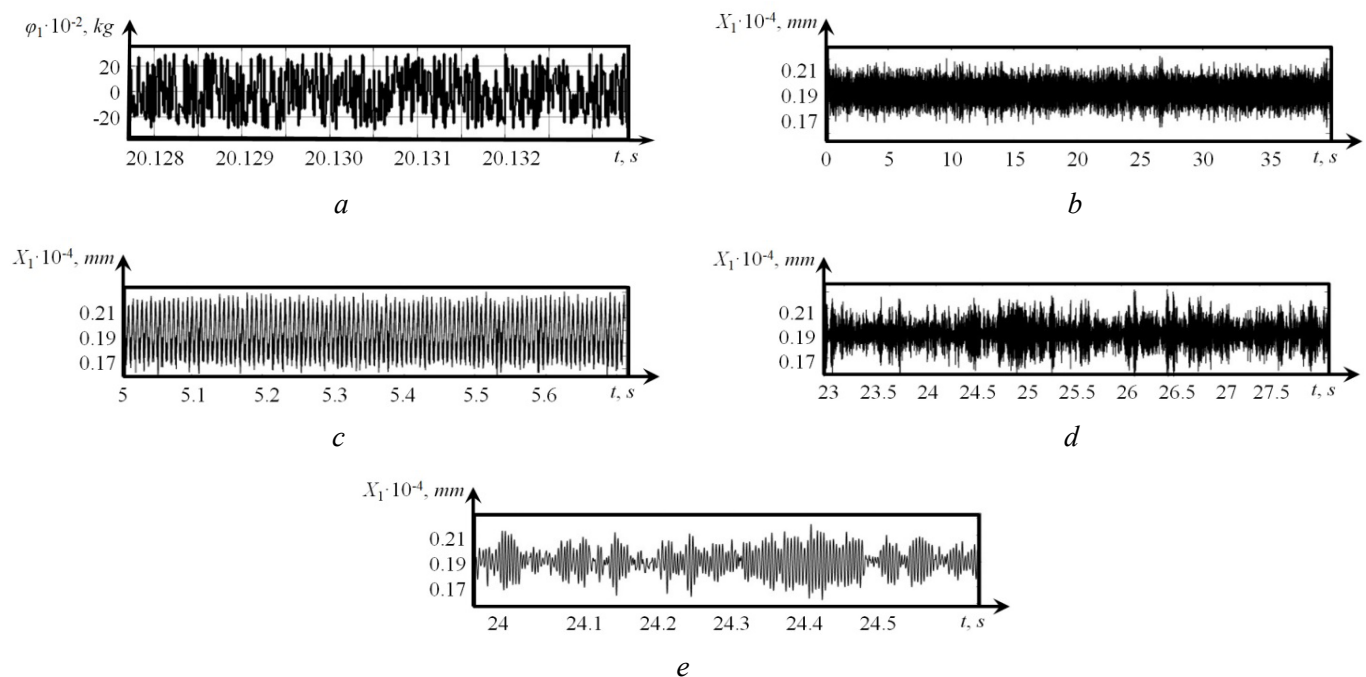


Fig. 3. Examples of trajectories:

a – power “white” noise; b, c – calculated deformations in two time scales; d, e – measured deformations in two time scales

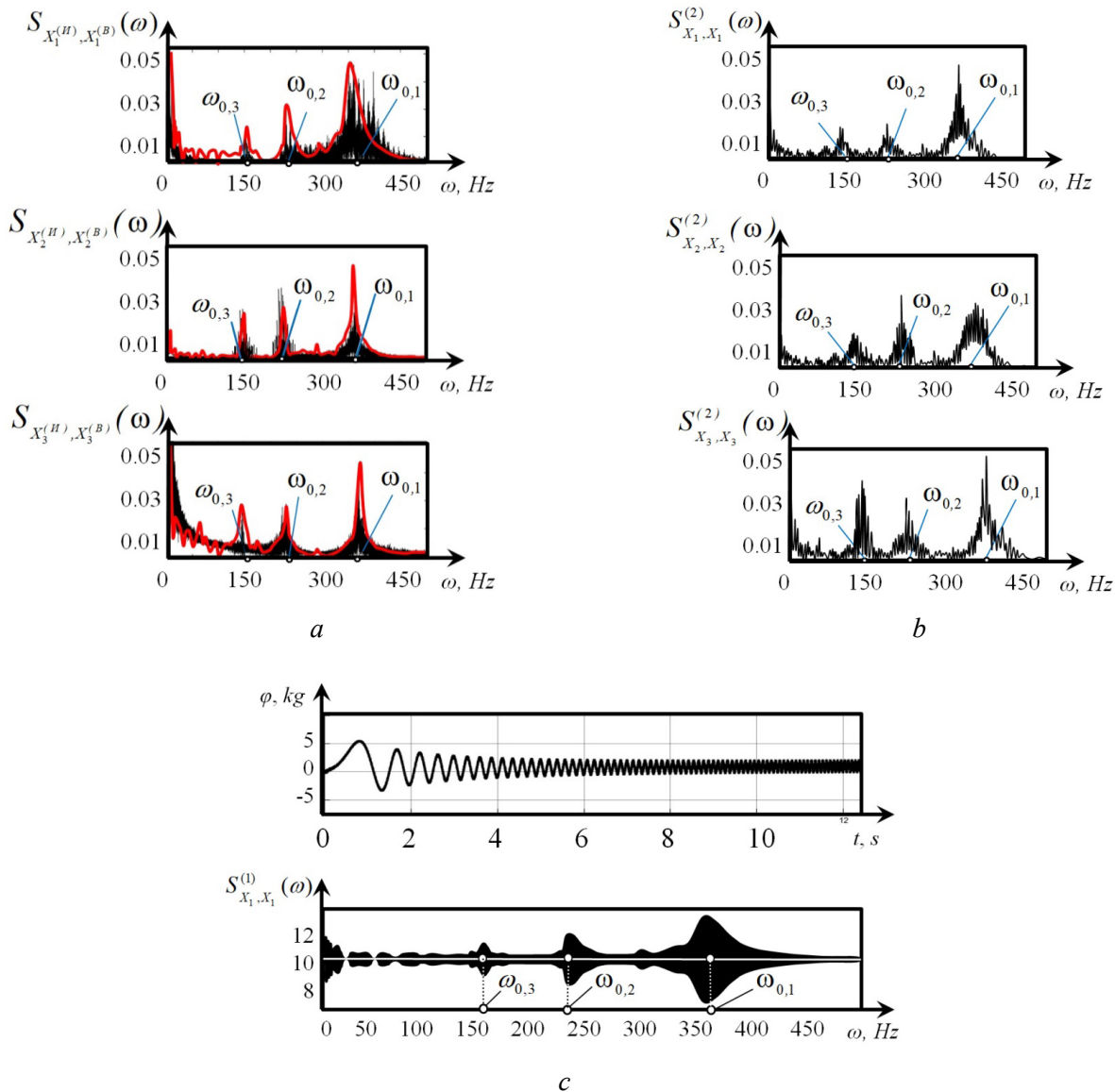


Fig. 4. Spectrums  $S_{X_S, X_S}^{(U)}(\omega)$  obtained on the basis of experiments (a); on the basis of digital sequence calculated after transformation by the model of power “white” noise  $S_{X_S, X_S}^{(2)}(\omega)$  (b); example of direct measurement of AFC on the model (c)

In fig. 4, a, the model-calculated spectra are highlighted in red color  $S_{X_1, X_1}^{(1)}(\omega)$ . The obtained sequences allow us to determine the coherence function  $K_{X_S, X_S}^{(U)}(\omega)$  (9). An example of this for various cutting speeds  $V_3$  and tool wear  $h$  is shown in fig. 5. There is also an example of evaluation of proximity of theoretical and experimental spectra  $\varphi_{X_S, X_S}^{(i)}(\omega)$ . The frequencies in which  $S_{X_S, X_S}^{(2)}(\omega) > 0.7$ , are highlighted on the curves  $S_{X_S, X_S}^{(2)}(\omega)$ . These results allow us to draw conclusions about the adequacy of the model (2). In the low-frequency range  $S_{X_S, X_S}^{(2)}(\omega) \rightarrow 1$ . As the frequency increases, there is a tendency to decrease  $S_{X_S, X_S}^{(2)}(\omega)$ , i.e. in the high-frequency region, usually lying outside the bandwidths of oscillating circuits  $S_{X_S, X_S}^{(2)}(\omega) \rightarrow 0$ .



An adequate description of deformations in the high-frequency region requires more complex models in which the interacting subsystems are systems with distributed parameters and physical interactions unrelated to the mechanics of the cutting process are additionally taken into account, for example, molecular-adhesion ones. The adequacy of the mathematical description of cutting dynamics also depends on the machining modes. It has been established that with increasing cutting speed there is an expansion of the frequency range in which the mathematical toolkit allows adequate evaluation of the deformations of the tool tip relative to the workpiece. This is indicated by the coherence function  $K_{X_S, X_S^{(U)}}^2(\omega)$ . It is enough to compare the graphs in fig. 5 *a*, *c* and *d*. In the region of frequencies close

to the resonances of the tool subsystem, the coherence function approaches unity. As wear increases, the frequency range in which mathematical modeling is adequate, also decreases. At frequencies equal or divisible to the rotational frequency of the workpiece  $\Omega$ , a sharp decrease in the coherence function was observed. The general trend of the uncertainty of the mathematical model is as follows: as the attenuation introduced by the dynamical system increases, the uncertainty of modeling the dynamical system as system (2) increases. This is also indicated by the estimation of the modeling error  $\wp_{X_S, X_S}^{(i)}(\omega)$  in the frequency domain (fig. 5, *e*).

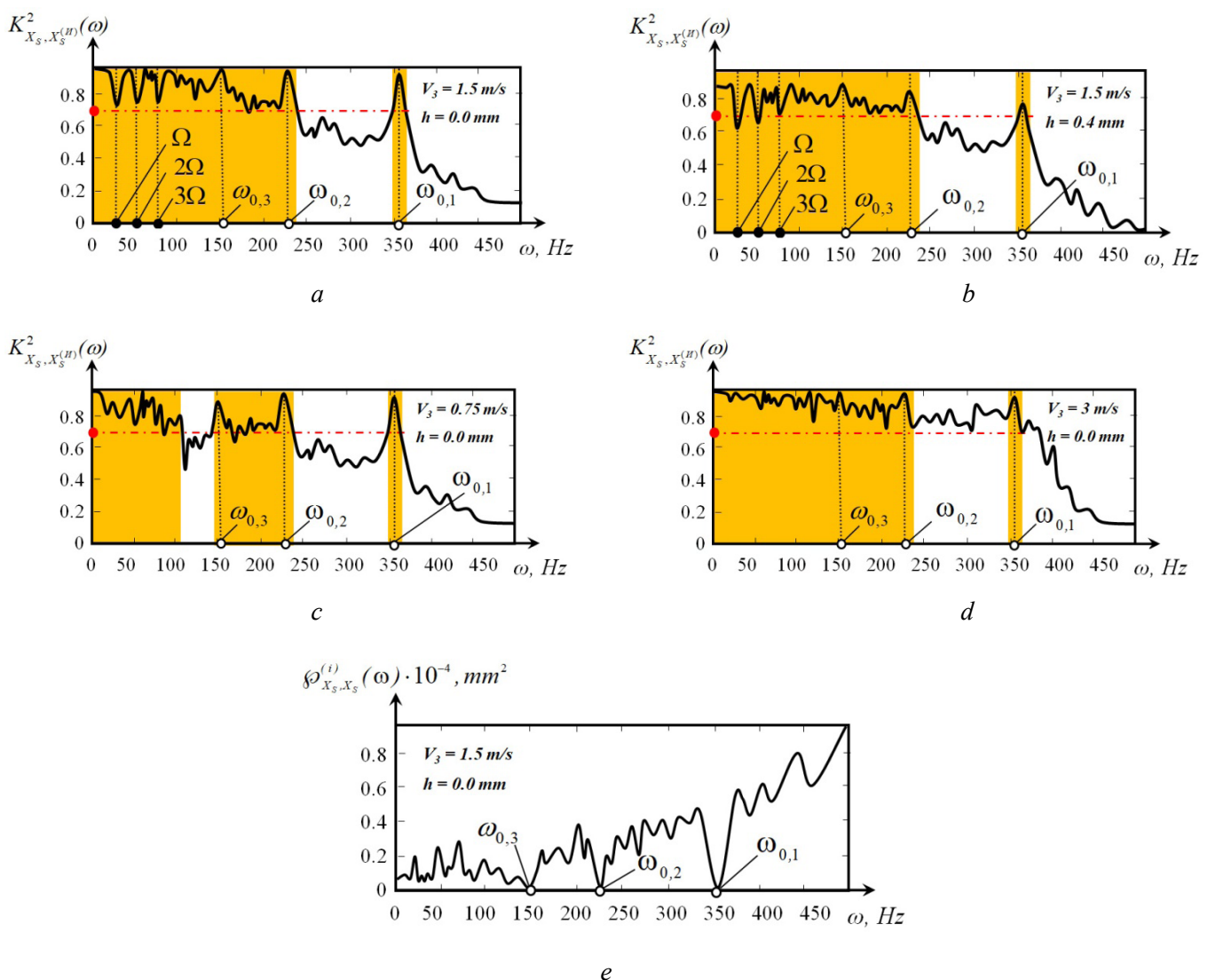


Fig. 5. Examples of coherence function variation and estimation of proximity of amplitude-frequency characteristics of the model and the real process

## Results and its discussion

The accuracy of the mathematical modeling of deformations does not guarantee the adequacy of its transformation into the part geometry. If it is possible to determine  $X(t)$ , the trajectories  $L^{(\Phi)}$ ,  $V^{(\Phi)}(t)$  are determined on the basis of (1) when  $L(t)$ ,  $V(t)$  are given. To analyze the adequacy of transformation forming motions into geometric topology, it is necessary to compare the two topologies  $\mathfrak{S}_c(L, X)$  and  $\mathfrak{S}(L, X)$  since the “skeletal” geometric topology is a direct geometric representation of the trajectory  $L^{(\Phi)}(t)$ ,  $V^{(\Phi)}(t)$  on the part surface. Note that if a geometric topology is specified, then any accepted engineering practice estimates of the geometric quality of the part can be calculated from it.

A profile and contour measuring station *T4HD* by *IMTS/Triebworx* (the error does not exceed  $0.01 \mu\text{m}$  in the range: diameter up to 200 mm and width of the controlled surface 20 mm) was used to measure the relief and surface morphology. The device allows measuring irregularities up to half of the circumference length. The measurement of  $X_1(t)$  and  $R(t)$  (fig. 6) allows spectral analysis of the vibrational displacements  $X_1(t)$  and profile function  $R(t)$  in the unity of the auto and cross spectrum, as well as the coherence function  $K_{X_1, R}^2(\omega)$ .

To evaluate the surface morphology, a three-dimensional microscope *Contour ELITE* (manufactured by *BRUKER*) was used, which allows obtaining photographs and surface relief with high resolution (in the horizontal plane of the order of 160 nm) (fig. 7). For vibration measurements, sensors made by *Bruel* and *Kjerr* and certified *AP35D* transducers with digital output were used. An integration operation was used to

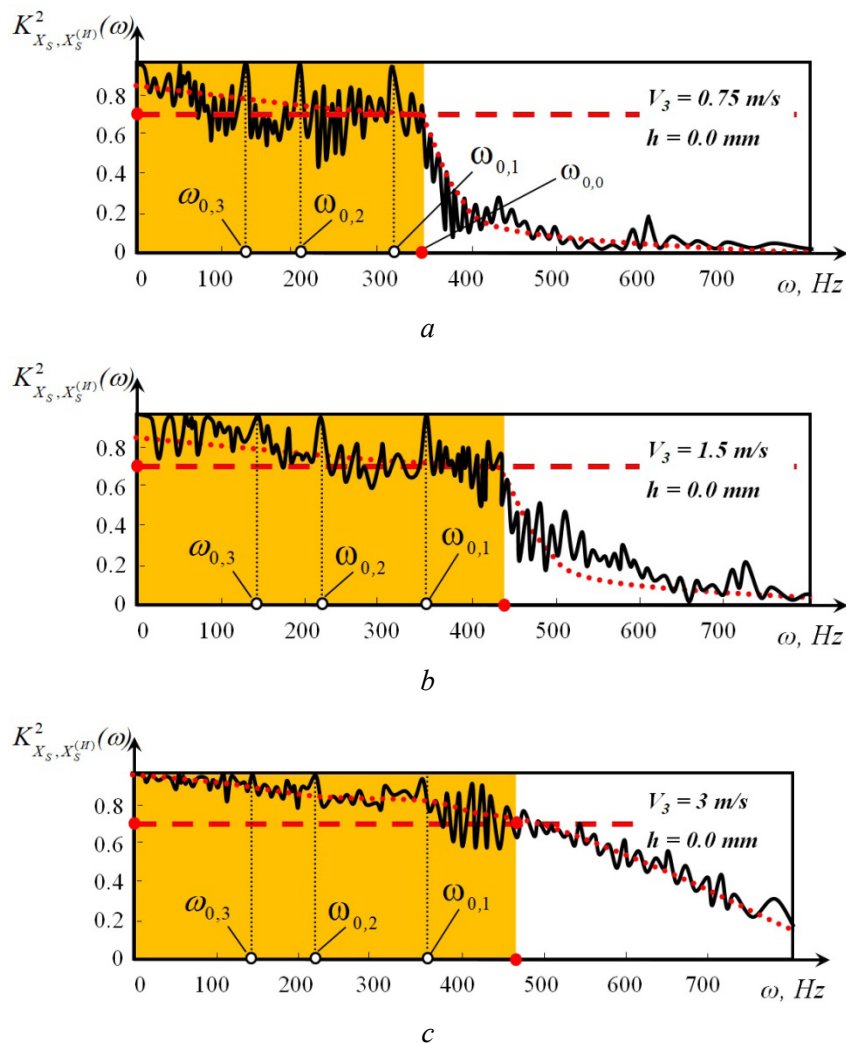


Fig. 6. Variation of coherence functions between vibrational displacements and profile function

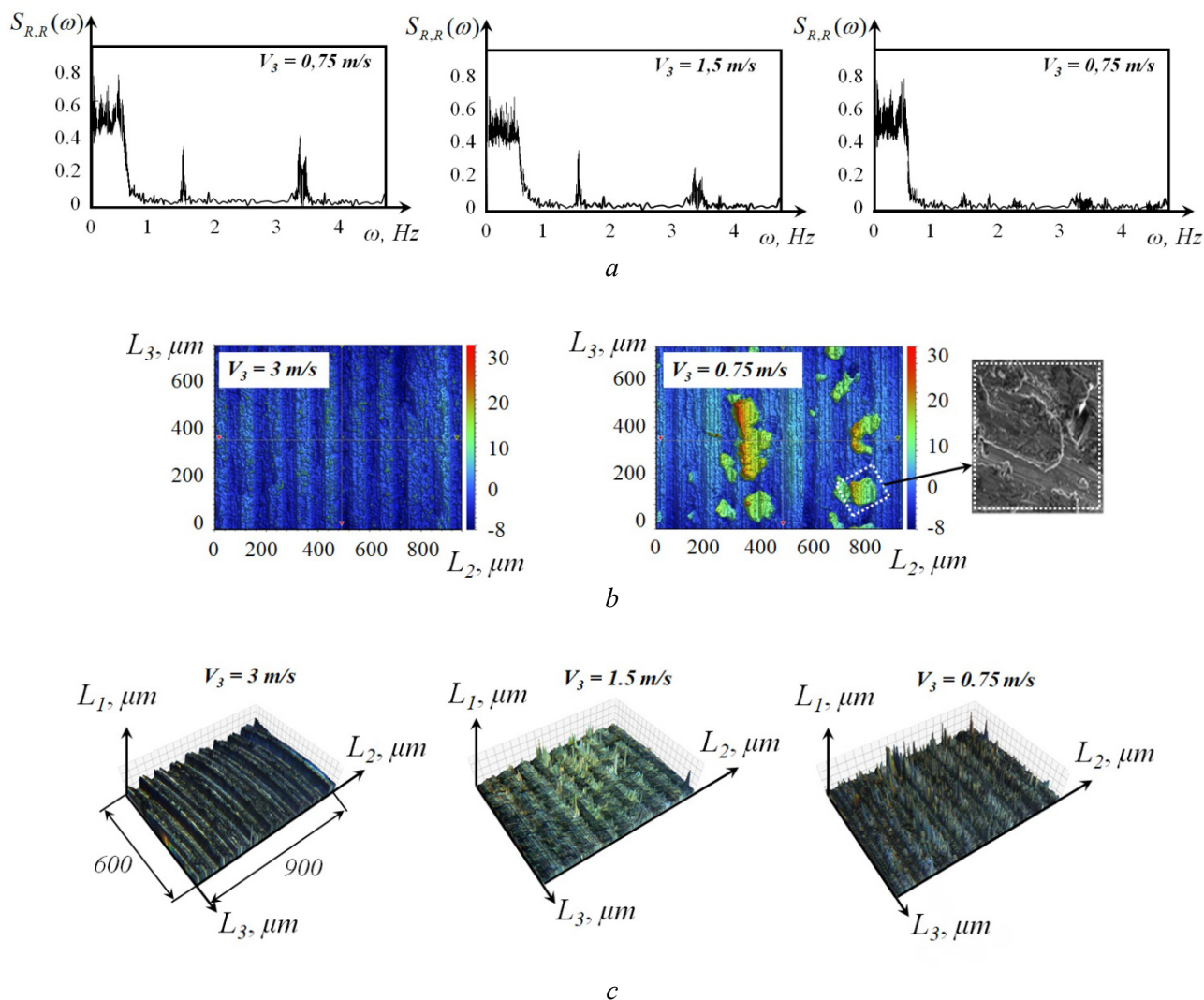


Fig. 7. Variation of micro surface morphology as a function of cutting speed:  
 a – dispersion normalized spectra of relief reduced to time sequence; b, c – surface morphologies

convert vibration velocities to displacements, with the removal of the trend caused by the uncertainty of the initial conditions. All instruments provide direct access to the computer memory for further automatic processing of information.

Let us first consider the change of  $K_{X_1,R}^2(\omega)$ . When machining a shaft, the profile function  $R(t)$  is represented as the deviation of the radius from the coordinate of the tool tip without taking into account elastic deformations  $L_2(0) = d/2$ . Rotational speed of the workpiece is  $\Omega = const$ . Therefore, the functions  $R(t)$  and  $R(L_3)$  differ by a constant coefficient, since  $L_3 = \pi d \Omega t$  (here  $\pi d \Omega$  is constant). As before, the conditions, under which the process is asymptotically stable and the strain variations are small, are considered. In this case, the coupling of  $X_1(t)$  and  $R(t)$  can be evaluated using the coherence function  $K_{X_1,R}^2(\omega)$ . Fig. 6 shows  $K_{X_1,R}^2(\omega)$  for the modes, at which the adequacy of the mathematical modeling of the system was analyzed (fig. 4). In fig. 6 the red dotted curves show the coherence functions averaged by moving average algorithms. The regions in which  $K_{X_1,R}^2(\omega) > 0,7$  are highlighted. The frequency region  $\omega \in (0, \omega_{0,0})$  is estimated as the range in which the formed relief is explained by  $L^{(0)}(t)$  trajectories.

Here the frequency  $\omega_{0,0}$  depends on the modes. It increases with increasing cutting speed and decreases with the development of tool wear, as well as with changes in all conditions under which the volume of

plastic deformation in the cutting zone increases. If we compare the coherence functions shown in fig. 5 and fig. 6, we can conclude that the topologies  $\mathfrak{S}_c(\mathbf{L}, \mathbf{X})$  and  $\mathfrak{S}(\mathbf{L}, \mathbf{X})$  are adequate. With the given mathematical tools it is possible to estimate only macro geometric characteristics. As far as surface roughness is concerned, a frequency range of up to 5.0 kHz, depending on the accuracy qualification, should be considered when forming it. In addition, molecular-mechanical interactions, plastic deformation processes and the dynamics of chip formation itself are of greater importance. If we follow *GOST 25142-82*, then irregularities within the length of the reference surface are in the frequency range in which  $K_{X_1, R}^2(\omega) > 0.7$  are located only in rough machining. To confirm this, it is sufficient to analyze the auto spectrum (fig. 7, a) calculated from the profile function measurement and the corresponding machined surface morphologies, which are obtained at three cutting speeds (fig. 7, b, c).

The geometrical topologies determined with the *Contour ELITE* microscope clearly show additional fine irregularities in the surface topography, which are formed in the vicinity of the tool tip trace obtained at low cutting speed (speed of 0.75 m/s). Such fine irregularities are practically absent at a cutting speed of 3.0 m/s. At the same time, the relief spectrum changes in the high-frequency region (fig. 7, a). In addition, the transition from relief at 3.0 m/s to relief at 0.75 m/s is characterized by instability of formation of additional deviations of relief different from the trace left by the tool.

## Conclusions

When creating a digital twin of the cutting process, one of the problems is to create a mathematical toolkit that can be used to reconstruct the geometry of the surface formed by cutting. The study considers the adequacy of the reconstructed geometrical topology  $\mathfrak{S}_c(\mathbf{L}, \mathbf{X})$ , obtained by calculating and/or measuring the trajectories of formative motions  $\mathbf{L}^{(\Phi)}(t)$ , as well as the real topology  $\mathfrak{S}(\mathbf{L}, \mathbf{X})$ . The real topology is represented as a function of the profile in the direction of cutting speed. The reconstructed topology  $\mathfrak{S}_c(\mathbf{L}, \mathbf{X})$  is based on the trajectory of forming motions, which represent the unity of the *TMAE*  $\mathbf{L}(t)$  defined by the *CNC* program and the trajectories of deformation displacements of the tool tip  $\mathbf{X}(t)$  relative to the workpiece. Two cases when the trajectory  $\mathbf{X}(t)$  is measured or calculated are considered.

In order to analyze the adequacy, the main attention is paid to the coherence function between the formative motions and the surface topography along the direction of tool motion. Examples of shaft surface morphology obtained by turning the shaft under different machining conditions and modes are also considered. The studies have shown, first, that the frequency range in which the reconstructed topology  $\mathfrak{S}_c(\mathbf{L}, \mathbf{X})$  adequately represents the real topology  $\mathfrak{S}(\mathbf{L}, \mathbf{X})$  is limited by the bandwidth of the adopted finite-dimensional model of the dynamic cutting system. In the examples under consideration, this band is  $\omega \in (0, \omega_{0,0})$ . Here, the upper frequency  $\omega_{0,0}$  depends not only on the bandwidth of the subsystems interacting through the cutting process, but also on the process modes. In the example under consideration, this range is limited to frequencies, at best in the range of 200–300 Hz. Under the conditions of the performed studies, there is a tendency of some expansion of the frequency range of adequate representation of the reconstructed topology of the real topology with increasing cutting speed. The  $\omega \in (0, \omega_{0,0})$  range decreases as tool wear develops and the amount of plastic deformation of the material in the cutting zone increases. By comparing the topology reconstructed from the measured vibration sequences  $\mathfrak{S}_c(\mathbf{L}, \mathbf{X})$  and the real topology  $\mathfrak{S}(\mathbf{L}, \mathbf{X})$  the frequency range  $\omega \in (0, \omega_{0,0})$  can be extended to 500 Hz. However, even in this case, only macro geometrical properties of the surface formed by cutting in the unity of dimensional accuracy and waviness can be adequately evaluated in the reconstructed topology. When estimating microrelief, more complex statistical estimations and more accurate measuring devices are required, which allow to significantly expanding the frequency range of modeled and measurable vibration sequences.

The performed analysis of elementary surface morphologies has shown that, when cutting speed decreases, additional deviations are formed in the vicinity of the trajectory formed by the tool tip, the physical nature of which is related to the plastic deformation of micro areas in the contact of auxiliary flanks





of the tool and the thermodynamics of cutting (fig. 7, *b* and *c*). In our opinion, depending on the cutting speed, it is necessary to take into account molecular-mechanical interactions, such as the formation and breaking of adhesive bonds. Its formation and breakage depend on the speed of tool movements relative to the workpiece. A number of key findings emerged from the study.

1. The quality of creating a digital twin of the cutting process on metal cutting machines depends on the depth of penetration of the models used in this process into the physics of interactions between the tool and the workpiece through the cutting zone.

2. Trajectories of forming motions of the tool relative to the workpiece, considered in the unity of the trajectories of the machine tool actuators and deformation displacements of the tool tip relative to the workpiece specified by the CNC system, adequately reflect the geometrical topology of the workpiece surface formed by cutting. However, the adequacy of such representation is limited by the frequency range, which depends, firstly, on the selective properties of the interacting subsystems on the side of the tool and the workpiece; secondly, it is limited by the possibility of measuring high-frequency vibrational displacements of the tool tip relative to the workpiece, as well as independent, not included in the dynamic cutting system, physical interactions in the cutting zone.

3. Mathematical modeling of the dynamic cutting system based on the mechanics of interaction between the tool and the workpiece allows to adequately predict the macro geometry of the part formed by cutting, but not the properties of surface roughness, much less the properties of the surface layer. For predicting microrelief, mathematical models that reveal the connection of trajectories of machine tool actuating elements taking into account elastic deformations into geometrical topology should be compositional. In addition to the mechanics of tool and workpiece interactions through the dynamic coupling formed by the cutting process, it is necessary to include thermodynamic and molecular interactions, as well as to take into account the plastic deformation of surface layers.

4. The present studies are limited to linearized models valid for small perturbations and for the case of stable trajectories. For large perturbations, it is necessary to additionally take into account nonlinear interaction effects, which will be analyzed in our next publications.

## References

1. Altintas Y. *Manufacturing automation: metal cutting mechanics, machine tool vibrations, and CNC design*. UK, Cambridge University Press, 2012. 366 p. DOI: 10.1017/CBO9780511843723.
2. Altintas Y., Brecher C., Weck M., Witt S. Virtual machine tool. *CIRP Annals*, 2005, vol. 54 (2), pp. 115–138. DOI: 10.1016/S0007-8506(07)60022-5.
3. Erkorkmaz K., Altintas Y., Yeung C.-H. Virtual computer numerical control system. *CIRP Annals*, 2006, vol. 55 (1), pp. 399–402. DOI: 10.1016/S0007-8506(07)60444-2.
4. Altintas Y., Kersting P., Biermann D., Budak E., Denkena B. Virtual process systems for part machining operations. *CIRP Annals*, 2014, vol. 63 (2), pp. 585–605. DOI: 10.1016/j.cirp.2014.05.007.
5. Gao W., Ibaraki S., Donmez M.A., Kono D., Mayer J.R.R., Chen Y.-L., Szipka K., Archenti A., Linares J.-M., Suzuki N. Machine tool calibration: Measurement, modeling, and compensation of machine tool errors International. *International Journal of Machine Tools and Manufacture*, 2023, vol. 187, p. 104017. DOI: 10.1016/j.ijmachtools.2023.104017.
6. Estman L., Merdol D., Brask K.-G., Kalhori V., Altintas Y. Development of machining strategies for aerospace components, using virtual machining tools. *New Production Technologies in Aerospace Industry*. Cham, Springer, 2014, pp. 63–68. DOI: 10.1007/978-3-319-01964-2\_9.
7. Kilic Z.M., Altintas Y. Generalized mechanics and dynamics of metal cutting operations for unified simulations. *International Journal of Machine Tools and Manufacture*, 2016, vol. 104, pp. 1–13. DOI: 10.1016/j.ijmachtools.2016.01.006.
8. Soori M., Arezoo B. Virtual machining systems for CNC milling and turning machine tools: a review. *International Journal of Engineering and Technology*, 2020, vol. 18, pp. 56–104.
9. Lin M.-T., Huang T.-Y., Tsai M.-S., Wu S.-K. Virtual simulation of five-axis machine tool with consideration of CNC interpolation, servo dynamics, friction, and geometric errors. *Journal of the Chinese Institute of Engineers*, 2017, vol. 40 (7), pp. 1–12. DOI: 10.1080/02533839.2017.1372221.





10. Lee C., Hwang S., Nam E., Min B. Identification of mass and sliding friction parameters of machine tool feed drive using recursive least squares method. *International Journal of Advanced Manufacturing Technology*, 2020, vol. 109, pp. 2831–2844. DOI: 10.1007/s00170-020-05858-x.
11. Duvedi R.K., Bedi S., Batish A., Mann S. A multipoint method for 5-axis machining of triangulated surface models. *Computer-Aided Design*, 2014, vol. 52, pp. 17–26. DOI: 10.1016/j.cad.2014.02.008.
12. Gan V.F., Fu J.Z., Shen H.Yu., Chen Z.Yu., Lin Z.V. Five-axis tool path generation in CNC machining of T-spline surfaces. *Computer-Aided Design*, 2014, vol. 52, pp. 51–63. DOI: 10.1016/j.cad.2014.02.013.
13. Kiswanto G., Hendriko H., Duk E. An analytical method for obtaining cutter workpiece engagement during a semi-finish in five-axis milling. *Computer-Aided Design*, 2014, vol. 55, pp. 81–93. DOI: 10.1016/j.cad.2014.05.003.
14. Tieng H., Yang H.C., Hung M.H., Cheng F.T. A novel virtual metrology scheme for predicting machining precision of machine tools. *IEEE International Conference on Robotics and Automation*. IEEE, 2013, pp. 264–269. DOI: 10.1109/ICRA.2013.6630586.
15. Wu D., Rosen D.W., Wang L., Schaefer D. Cloud-based design and manufacturing: a new paradigm in digital manufacturing and design innovation. *Computer-Aided Design*, 2015, vol. 59, pp. 1–14. DOI: 10.1016/j.cad.2014.07.006.
16. Yang J., Guo G. Design a new manufacturing model: cloud manufacturing. *Proceedings of the 2012 International Conference on Cybernetics and Informatics*. New York, Springer, 2014, pp. 1597–1606. DOI: 10.1007/978-1-4614-3872-4\_205.
17. Sulitka M., Kolar P., Sveda J., Smolik J. Strategy for implementing predictive process-oriented machine tool digital twins. *MM Science Journal*, 2022, vol. 10, pp. 5954–5961. DOI: 10.17973/mmsj.2022\_10\_2022121.
18. Kabaldin Yu.G., Shatagin D.A., Anosov M.S., Kuzmishina A.M. Razrabotka tsifrovogo dvoynika stanka s ChPU na osnove metodov mashinnogo obucheniya [Development of digital twin of CNC unit based on machine learning methods]. *Vestnik Donskogo gosudarstvennogo tekhnicheskogo universiteta = Vestnik of Don State Technical University*, 2019, no. 19 (1), pp. 45–55. DOI: 10.23947/1992-5980-2019-19-1-45-55.
19. Kabaldin Yu.G., Shatagin D.A., Kuzmishina A.M. Razrabotka tsifrovogo dvoynika rezhushchego instrumenta dlya mekhanooobratyvayushchego proizvodstva [The development of a digital twin of a cutting tool for mechanical production]. *Izvestiya vysshikh uchebnykh zavedenii. Mashinostroenie = Proceedings of Higher Educational Institutions. Machine Building*, 2019, no. 4, pp. 11–17. DOI: 10.18698/0536-1044-2019-4-11-17.
20. Pantyukhin O.V., Vasin S.A. Tsifrovoi dvoynik tekhnologicheskogo protsessa izgotovleniya izdelii spetsial'nogo naznacheniya [Digital double of the technological process of manufacturing special-purpose products]. *Stankoinstrument*, 2021, no. 1 (22), pp. 56–59. DOI: 10.22184/2499-9407.2021.22.1.56.58. (In Russian).
21. Burlachenko O.V., Oganesyana O.V. Tsifrovaya tekhnologiya vybora i transformatsii informatsii dlya upravleniya i podderzhki zhiznennogo tsikla izdeliya [Digital technology of information selection and transformation for product life cycle management and support]. *Izvestiya vysshikh uchebnykh zavedenii. Mashinostroenie = Proceedings of Higher Educational Institutions. Machine Building*, 2023, no. 3 (756), pp. 3–13. DOI: 10.18698/0536-1044-2023-3-3-13.
22. Zakovorotny V.L., Pham D.T., Nguyen X.C., Ryzhkin M.N. Modelirovanie dinamicheskoi svyazi, formiruemoi protsessom tocheniya, v zadachakh dinamiki protsessa rezaniya (pozitsionnaya svyaz') [Dynamic coupling modeling formed by turning in cutting dynamics problems (positional coupling)]. *Vestnik Donskogo gosudarstvennogo tekhnicheskogo universiteta = Vestnik of Don State Technical University*, 2011, vol. 11, no. 3 (54), pp. 301–311.
23. Zakovorotny V.L., Flek M.B. *Dinamika protsessa rezaniya. Sinergeticheskii podkhod* [The dynamics of the cutting process. Synergistic approach]. Rostov-on-Don, Terra Publ., 2005. 880 p.
24. Ryzhkin A.A. *Sinergetika iznashivaniya instrumental'nykh materialov pri lezviinoi obrabotke* [Synergetics of tool wear in cutting edge treatment]. Rostov-on-Don, Don State Technical University Publ., 2019. 289 p. ISBN 978-5-7890-1669-5.
25. Starkov V.K. *Fizika i optimizatsiya rezaniya materialov* [Physics and optimization of cutting materials]. Moscow, Mashinostroenie Publ., 2009. 639 p.
26. Sankin Yu.N., Sankin N.Yu. *Ustoichivost' tokarnykh stankov pri nelineinoi kharakteristike protsessa rezaniya* [Stability of lathes with nonlinear characteristics of the cutting process]. Ulyanovsk, UISTU Publ., 2008. 137 p.
27. Hahn R.S. On the theory of regenerative chatter in precision grinding operation. *Transactions of American Society of Mechanical Engineers*, 1954, vol. 76, pp. 356–260.
28. Tobias S.A., Fishwick W. Theory of regenerative machine tool chatter. *The Engineer*, 1958, vol. 205, pp. 199–203.



29. Merritt H.E. Theory of self-excited machine-tool chatter: contribution to machine-tool chatter research – 1. *Journal of Engineering for Industry*, 1965, vol. 87 (4), pp. 447–454. DOI: 10.1115/1.3670861.
30. Zhou G., Yuan M., Feng F., Han Z., Song X., Wang X., Feng P., Zhang M. A new algorithm for chatter quantification and milling instability classification based on surface analysis. *Mechanical Systems and Signal Processing*, 2023, vol. 204, p. 110816. DOI: 10.1016/j.ymssp.2023.110816.
31. Kudinov V.A. *Dinamika stankov* [Dynamics of machine tools]. Moscow, Mashinostroenie Publ., 1967. 359 p.
32. Tlustý J., Poláček A., Danek C., Spacek J. *Selbsterregte Schwingungen an Werkzeugmaschinen*. Berlin, Verlag Technik, 1962. 320 p.
33. Tlustý J., Ismail F. Basic non-linearity in machining chatter. *CIRP Annals*, 1981, vol. 30, pp. 299–304.
34. Hanna N.H., Tobias S. A theory of nonlinear regenerative chatter. *Journal of Engineering for Industry*, 1974, vol. 96 (1), pp. 247–255. DOI: 10.1115/1.3438305.
35. Wahi P., Chatterjee A. Self-interrupted regenerative metal cutting in turning. *International Journal Non-Linear Mechanics*, 2008, vol. 43, pp. 111–123. DOI: 10.1016/j.ijnonlinmec.2007.10.010.
36. Stépán G., Szalai R., Insperger T. Nonlinear dynamics of high-speed milling subjected to regenerative effect. *Nonlinear Dynamics of Production Systems*. Weinheim, Wiley-VCH, 2004, pp. 111–127. DOI: 10.1002/3527602585.ch7.
37. Stépán G., Insperger T., Szalai R. Delay, parametric excitation, and the nonlinear dynamics of cutting processes. *International Journal of Bifurcation and Chaos*, 2005, vol. 15 (9), pp. 2783–2798. DOI: 10.1142/S0218127405013642.
38. Brissaud D., Gousskov A., Guibert N., Rech J. Influence of the ploughing effect on the dynamic behavior of the self-vibratory drilling head. *CIRP Annals. Manufacturing Technology*, 2008, pp. 385–388. DOI: 10.1016/j.cirp.2008.03.101.
39. Gousskov A., Gousskov M., Lorong Ph., Panovko G. Influence of the clearance face on the condition of chatter selfexcitation during turning International. *Journal of Machining and Machinability of Materials*, 2017, vol. 19 (1), pp. 17–39. DOI: 10.1504/IJMMM.2017.10002088.
40. Voronov S.A., Kiselev I.A. Nelineinye zadachi dinamiki protsessov rezaniya [Nonlinear problems of cutting process dynamics]. *Mashinostroenie i inzhenernoe obrazovanie = Mechanical Engineering and Engineering Education*, 2017, no. 2 (51), pp. 9–23.
41. Gousskov A.M., Gousskov M.A., Dinh Dyk T., Panovko G.Ya. Modeling and investigation of the stability of a multicutter turning process by a trace. *Journal of Machinery Manufacture and Reliability*, 2018, vol. 47 (4), pp. 317–323. DOI: 10.3103/S1052618818040052. Translated from *Problemy mashinostroeniya i nadezhnosti mashin*, 2018, no. 4, pp. 19–27. DOI: 10.31857/S023571190000533-7.
42. Gousskov A.M., Panovko G.Ya., Shokhin A.E. Dynamics of the rotor system of a vibrational-centrifugal separator with an elastic vibration limiter. *Journal of Machinery Manufacture and Reliability*, 2023, vol. 51 (8), pp. 733–745. DOI: 10.3103/S105261882208009X.
43. Veits V.L., Vasilkov D.V. Zadachi dinamiki, modelirovaniya i obespecheniya kachestva pri mekhanicheskoi obrabotke malozhestkikh zagotovok [Problems of dynamics, modeling and quality assurance in machining of low-rigid workpieces]. *STIN*, 1999, no. 6, pp. 9–13. (In Russian).
44. Altintas Y., Budak E. Analytical prediction of stability lobes in milling. *CIRP Annals. Manufacturing Technology*, 1995, vol. 44 (1), pp. 357–362. DOI: 10.1016/S0007-8506(07)62342-7.
45. Altintas Y., Weck M. Chatter stability of metal cutting and grinding. *CIRP Annals. Manufacturing Technology*, 2004, vol. 53 (2), pp. 619–642. DOI: 10.1016/S0007-8506(07)60032-8.
46. Insperger T., Stépán G. Semi-discretization method for delayed systems. *International Journal for Numerical Methods in Engineering*, 2002, vol. 55 (5), pp. 503–518. DOI: 10.1002/nme.505.
47. Zakovorotnyi V.L., Gvindjiliya V.E. Vliyanie fluktuatsii na ustoychivost' formoobrazuyushchikh traektorii pri tochenii. *Izvestiya vysshikh uchebnykh zavedenii. Severo-Kavkazskii region. Tekhnicheskie nauki = University News. North-Caucasian Region. Technical Sciences Series*, 2017, no. 2 (194), pp. 52–61.
48. Zakovorotny V.L., Lukyanov A.D., Gubanova A.A., Hristoforova V.V. Bifurcation of stationary manifolds formed in the neighborhood of the equilibrium in a dynamic system of cutting. *Journal of Sound and Vibration*, 2016, vol. 368, pp. 174–190. DOI: 10.1016/j.jsv.2016.01.020.
49. Murashkin L.S., Murashkin S.L. *Prikladnaya nelineinaya mekhanika stankov* [Applied nonlinear mechanics of machines]. Leningrad, Mashinostroenie Publ., 1977. 192 p.
50. Grabec I. Chaos generated by the cutting process. *Physics Letters*, 1986, vol. 117, pp. 384–386. DOI: 10.1016/0375-9601(86)90003-4.



51. Wiercigroch M., Budak E. Sources of nonlinearities, chatter generation and suppression in metal cutting. *Philosophical Transactions of the Royal Society A*, 2001, vol. 359 (1781), pp. 663–693. DOI: 10.1098/rsta.2000.0750.
52. Wiercigroch M., Krivtsov A.M. Frictional chatter in orthogonal metal cutting. *Philosophical Transactions of the Royal Society A*, 2001, vol. 359 (1781), pp. 713–738. DOI: 10.1098/rsta.2000.0752.
53. Rusinek R., Wiercigroch M., Wahi P. Influence of tool flank forces on complex dynamics of a cutting process. *International Journal of Bifurcation and Chaos*, 2014, vol. 24 (9), pp. 189–201. DOI: 10.1142/S0218127414501156.
54. Rusinek R., Wiercigroch M., Wahi P. Modeling of frictional chatter in metal cutting. *International Journal of Mechanical Sciences*, 2014, vol. 89, pp. 167–176. DOI: 10.1016/j.ijmecsci.2014.08.020.
55. Shao Y.-F., Ding H. Evaluation of gravity effects on the vibration of fluid-conveying pipes. *International Journal of Mechanical Sciences*, 2023, vol. 248 (5), p. 108230. DOI: 10.1016/j.ijmecsci.2023.108230.
56. Zakovorotny V.L., Gubanov A.A., Lukyanov A.D. Attractive manifolds in end milling. *Russian Engineering Research*, 2017, vol. 37 (2), pp. 158–163.
57. Zakovorotnyi V.L., Bykador V.S. Cutting-system dynamics. *Russian Engineering Research*, 2016, vol. 36 (7), pp. 591–598. DOI: 10.3103/S1068798X16070182.
58. Zakovorotny V.L., Pham D.T., Pham T.H. Parametricheskie yavleniya pri upravlenii protsessami obrabotki na stankakh [Parametrical phenomena under on-machine process control]. *Vestnik Donskogo gosudarstvennogo tekhnicheskogo universiteta = Vestnik of Don State Technical University*, 2012, vol. 12, no. 7, pp. 52–61.
59. Zakovorotny V.L., Gvindjiliya V.E. Vliyanie vibratsii na traektorii formoobrazuyushchikh dvizhenii instrumenta pri tochenii [The influence of the vibration on the tool shape-generating trajectories when turning]. *Obrabotka metallov (tekhnologiya, oborudovanie, instrumenty) = Metal Working and Material Science*, 2019, vol. 21, no. 3, pp. 42–58. DOI: 10.17212/1994-6309-2019-21.3-42-58.
60. Zakovorotny V.L., Gvindzhiliya V.E. Influence of spindle wobble in turning on the workpiece's surface topology. *Russian Engineering Research*, 2018, vol. 38, pp. 818–823. DOI: 10.3103/S1068798X18100192.
61. Zakovorotny V., Pham D., Nguyen X. Modelirovanie i identifikatsiya inertsionnykh i dissipativnykh svoystv podsystem rezhushchego instrumenta i zagotovki pri tochenii [Modeling and identification of inertial and dissipative properties of subsystems of cutting tool and workpiece in turning]. *Vestnik Donskogo gosudarstvennogo tekhnicheskogo universiteta = Vestnik of Don State Technical University*, 2010, vol. 10 (8), pp. 1165–1178.

## Conflicts of Interest

The authors declare no conflict of interest.

© 2024 The Authors. Published by Novosibirsk State Technical University. This is an open access article under the CC BY license (<http://creativecommons.org/licenses/by/4.0>).